Photochemical & Photobiological Sciences

PAPER

Cite this: *Photochem. Photobiol. Sci.*, 2016, **15**, 928

Photochemically-assisted synthesis and photophysical properties of difluoroboronated β-diketones with fused four-benzene-ring chromophores, chrysene and pyrene†

Michitaka Mamiya,[a] Yurie Suwa,[a] Hideki Okamoto[b] and Minoru Yamaji*[c]

Received 31st March 2016,
Accepted 2nd June 2016

DOI: 10.1039/c6pp00089d

www.rsc.org/pps

We investigated the photophysical properties of difluoroboronated β-diketones (BF_2DK) with chrysene and pyrene skeletons (ChB and PyB, respectively) in solution and in the solid state. Acetylchrysenes, as the key precursors to ChBs, were photochemically prepared from the corresponding (acetylphenyl)naphthylethenes by means of a modified photocyclization method. The absorption and emission spectra of the BF_2DKs were obtained in chloroform and acetonitrile, and the quantum yields and lifetimes of the fluorescence were determined. Excimeric fluorescence from PyB was absent even in highly concentrated solution. Based on the Lippert–Mataga analysis of the absorption and fluorescence features, the photophysical properties of the ChBs were discussed in comparison with those of PyB. The fluorescence states of the studied BF_2DKs are shown to be of a charge-transfer character. The fluorescence quantum yields decrease with increasing the solvent polarity due to the enhanced internal conversion process. The fluorescence quantum yields in the solid state of the studied BF_2DKs were determined, and it was found that PyB is fluorescent, whereas the fluorescence quantum yields of the ChBs depend on the substituted position of the chrysene moiety.

1. Introduction

Aromatic difluoroboronated β-diketones (BF_2DKs) are known to show intense fluorescence in solution and in the solid state although they have small size chromophores and no heavy metal atoms.[1–3] The BF_2DKs of dibenzoylmethanes were initially studied as photochemical reagents,[4–9] but recently, much attention has been paid to them from the viewpoints of two-photon absorbing molecules,[10,11] near-IR probes,[12,13] photochromic molecules,[13] oxygen[14] and mechanical sensors,[15] mechanochromic luminescence materials,[16] semiconductors,[17,18] and conjugated polymers.[19–25] Recently, BF_2DKs improved by adopting expanded π-electron systems have been reported.[26–31] It is vigorously required to tune their photophysical features, such as fluorescence quantum yields and wavelengths, by modifying the chromophores of BF_2DK in order to apply them to luminescence devices. The fluorescence quantum yields of BF_2DKs with the naphthyl and anthryl chromophores are reported to be, respectively, *ca.* 0.5 and 0.3 in solution.[32] Anthracene has a linear benzene ring alignment (acene), whereas phenanthrene, chrysene, and picene have a zigzag benzene ring alignment (phenacene). Recently, attention has been paid to phenacenes as potential materials for fluorophores and semi- and super-conductors.[33–39] In this context, we investigated the photophysical properties of BF_2DKs with phenanthrene, which has the same number of benzene rings as anthracene, in a previous report.[40] Interestingly, they showed fluorescence quantum yields of *ca.* 0.8 in solution, which were much larger than that (0.3)[32] of the BF_2DK incorporating an anthracene chromophore. From these facts, we hypothesized that employing phenacene moieties as the chromophores of BF_2DK could be a strategy for enhancing the fluorescence quantum yields. In the present study, we paid attention to chrysene and pyrene with four benzene rings as the BF_2DK chromophores. Chrysene, as the second smallest member of the phenacene family, was thus adopted as a chromophore of the BF_2DKs. For comparison with chrysene, we also employed pyrene, which is a typical fluorophore, in

[a]*Education Program of Materials and Bioscience, Graduate School of Science and Engineering, Gunma University, Kiryu, Gunma 376-8515, Japan*
[b]*Division of Earth, Life, and Molecular Sciences, Graduate School of Natural Sciences and Technology, Okayama University, Okayama 700-8530, Japan*
[c]*Division of Molecular Science, Graduate School of Science and Engineering, Gunma University, Kiryu, Gunma 376-8515, Japan. E-mail: yamaji@gunma-u.ac.jp*

† Electronic supplementary information (ESI) available: Procedures for preparing the compounds, experimental details, absorption and fluorescence spectra in MeCN and DMSO, decay profiles of fluorescence, data for the Lippert–Mataga analysis, transient absorption spectra in MeCN, results of the DFT calculations, including calculated absorption spectra, tables of atom coordinates for the optimized geometries, and ^{1}H and ^{13}C NMR spectra. See DOI: 10.1039/c6pp00089d

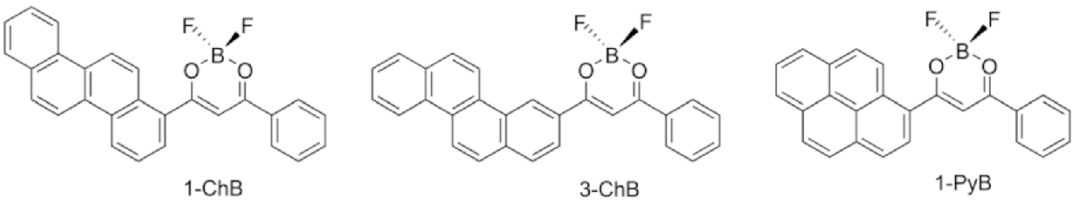

Chart 1 Molecular structures and abbreviations of the BF_2DKs used in this study.

order to understand effects of the alignment of the four benzene rings on the fluorescence properties of BF_2DKs. It is well-known that pyrene emits excimeric fluorescence in concentrated solution.[41] Thus, it was of an additional interest to us to know whether excimer fluorescence is observable from the BF_2DK incorporating a pyrene chromophore, which has not been synthesized before.

In the present research, we prepared BF_2DK with the chrysene substituted at various positions and pyrene moieties (see Chart 1) and studied their fluorescence behavior. The synthesis of aromatic β-diketones as ligands BF_2DK was readily performed by condensation of an appropriate acetyl aromatic compound with an aromatic ester. The chrysene skeletons could be photochemically prepared from diarylethene by using the Mallory method[42] and by diarylethane with a sensitization method.[35] We adapted the Mallory method for preparing acetylchrysenes in the present synthesis for the BF_2DKs with chrysene moieties because it is one of the most common methodologies for constructing a phenacene skeleton.[42] The emission features of the prepared four-benzene-ring BF_2DK were investigated based on fluorescence and on transient absorption measurements with the aid of theoretical computations.

2. Experimental

2.1. General

NMR spectra were recorded on 400- and 600 MHz spectrometers. Melting points were obtained with a micro melting point apparatus.

2.2. Materials

Acetonitrile (MeCN) for the spectral measurements was purified by distillation. Benzene, carbon tetrachloride, toluene, chloroform (spectroscopic grade), diethyl ether, THF, DMSO, dichloromethane (spectroscopic grade), and ethanol (EtOH, spectroscopic grade) were used as the solvents without further purification for the spectral measurements.

2.3. Absorption, emission, and transient absorption measurements

Absorption spectra were recorded on a U-best 50 (JASCO) spectrophotometer while the emission spectra were recorded on a Hitachi F-4010 fluorescence spectrophotometer. Quantum yields of the fluorescence and the fluorescence spectra of the samples in the solid states were obtained with a Hamamatsu Photonics C9920-02 absolute PL quantum yields measurement system. Fluorescence lifetimes (τ_f) were determined with a Hamamatsu Photonics Tau time-correlated single-photon counting fluorimeter system. Samples in a quartz cell with a 1 cm or 1 mm path length were prepared in the dark, and Ar-purged when necessary. A 250 W xenon lamp ($\lambda > 310$ nm) was employed as a light source upon steady-state photolysis, while the fourth harmonics (266 nm) laser pulses (7 mJ per pulse) from the Nd:YAG laser system (12 mJ per pulse, Lotis-TII, LT-2137) were used as the excitation laser light source. The details of the detection system for the time profiles of the transient absorption have been reported elsewhere.[43] Transient absorption spectra were obtained using a Unisoku USP-T1000-MLT system, which provides a transient absorption spectrum with one laser pulse. The obtained transient spectral data were analyzed using the least-squares best-fitting method. The temporal data of the absorbance changes were analyzed by using the least-squares best-fitting method.

2.4. Theoretical calculations

The calculation was carried out at the DFT level, using the Gaussian 09 software package.[44] The geometries of the BF_2DKs were fully optimized by using the 6-31G(d) basis set at the B3LYP method in vacuum and by considering the solvation effects of the $CHCl_3$ and MeCN included by self-consistent reaction field (SCRF) theory using the conductor-like polarizable continuum model (CPCM). Atom coordinates for the optimized geometries are deposited in the ESI.† TD-DFT calculations were performed at the TD B3LYP/6-31G(d) level using the optimized geometries.

3. Results and discussion

Acetyl aromatic compounds are the key precursors to the desired BF_2DKs. 1-Acetylpyrene **13** was commercially available, whereas 1- and 3-acetylchrysenes (**8** and **9**, respectively) were synthesized by the photocyclization of acetal-protected (acetylphenyl)naphthylethenes. The synthetic route to **8** and **9** is illustrated in Scheme 1.

Diarylethenes **2** and **3** were prepared by the Wittig reaction of phosphonium salt **1** and the corresponding acetylbenzaldehyde in a quantitative yield. We performed acetal protection of the acetyl group in compounds **2** and **3** to afford compounds **4** and **5**, respectively, since they did not undergo photocyclization

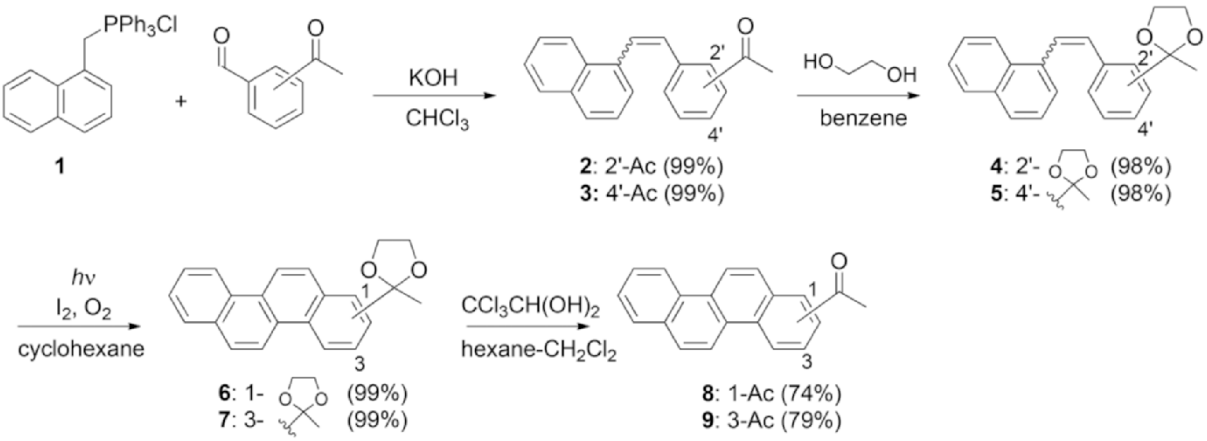

Scheme 1 Synthetic procedures for the acetylchrysenes **8** and **9**.

in the presence of iodine in aerated cyclohexane. For the photocyclization of compounds **4** and **5**, a continuous flow technique was used,[45] thus, compounds **4** and **5** were subjected to photocyclization to form the corresponding chrysene derivatives **6** and **7**, respectively, in quantitative yields. Deprotection of the acetals **6** and **7** by chloral hydrate[46] provided the desired acetylchrysenes **8** and **9**, respectively.

The desired β-diketones **11**, **12**, and **13** were prepared in moderate to good yields by the Claisen condensation of the acetylchrysenes **8** and **9**, and acetylpyrene **10**, respectively, with methyl benzoate in the presence of NaH (Scheme 2).

Finally, the desired BF_2DKs were successfully prepared *via* the reaction between boron trifluoride diethyl etherate and the corresponding diketones **11–13**. The novel compounds were well characterized by NMR spectroscopy as well as by high-resolution mass spectrometry. The precise synthetic procedures and analytical data are described in the ESI.†

Fig. 1 shows the absorption and emission spectra of the prepared BF_2DKs in $CHCl_3$.

The absorption spectra of the BF_2DKs have large molar absorption coefficients (ε) in the magnitude of 10^4 dm^3 mol^{-1} cm^{-1} (see Table 1), which are typical for π–π* transitions. We performed photolysis of the BF_2DKs in Ar-purged $CHCl_3$ using a xenon lamp (λ > 310 nm). No changes in the absorption

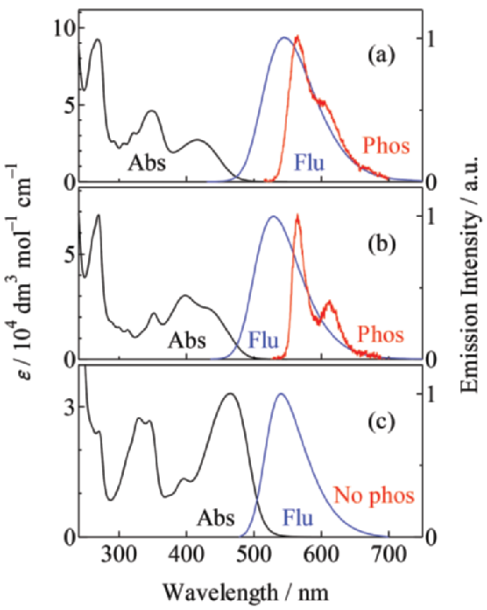

Fig. 1 Absorption (black) and fluorescence (blue) spectra in $CHCl_3$ at 295 K and the phosphorescence spectra (red) in EtOH at 77 K obtained for 1-ChB (a), 3-ChB (b), and 1-PyB (c). Phosphorescence from 1-PyB was not observed in EtOH at 77 K. The emission spectra are not corrected.

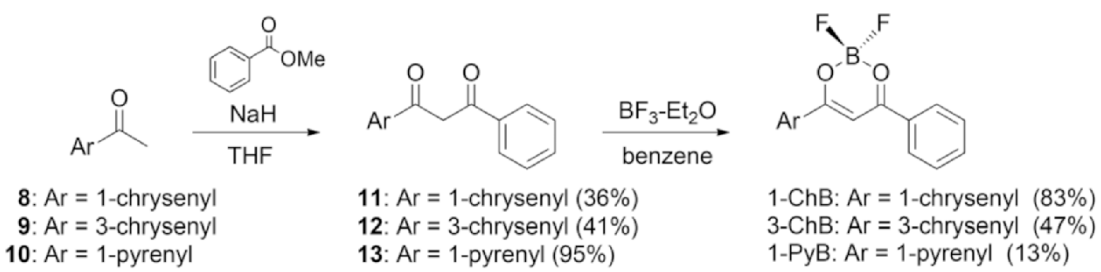

Scheme 2 Preparation of BF_2DKs.

Table 1 Photophysical parameters of BF_2DKs obtained in $CHCl_3$

Compound	ε/dm^3 mol^{-1} cm^{-1} (λ_{abs}/nm)	λ_{flu} [a]/nm	Φ_f [a]	τ_f [a]/ns	k_f [a,b]/10^7 s^{-1}	Φ_{nr} [a,c]	k_{nr} [a,d]/10^7 s^{-1}	E_T [e]/kcal mol^{-1}	λ_{flu}^{powder} [f]/nm	Φ_f^{powder} [f]	τ_T [a]/μs
1-ChB	93 000 (269), 32 000 (348), 19 000 (416)	545 (600)	0.79 (0.04)	8.2 (0.95)	9.6 (4.2)	0.21 (0.96)	2.6 (101)	50.6	540	0.25	20.7 (N/D)
3-ChB	68 000 (270), 21 000 (353), 29 000 (397)	529 (586)	0.88 (0.30)	6.5 (5.0)	13.5 (6.0)	0.12 (0.70)	1.8 (14.0)	50.6	630	0.06	23.0 (21.5)
1-PyB	29 000 (330), 33 000 (463)	540 (564)	0.86 (0.04)	4.7 (0.40 (87%), 2.5 (13%))	18.0 (N/D)	0.14 (0.96)	3.0 (N/D)	N/D	690	0.20	56.3 (N/D)

[a] Data in parentheses were obtained in MeCN. N/D indicates not determined. [b] Determined by the equation, $k_f = \Phi_f \tau_f^{-1}$. [c] Determined by the equation, $\Phi_{nr} = 1 - \Phi_f$. [d] Determined by the equation, $k_{nr} = \Phi_{nr} \tau_f^{-1}$. [e] Determined from the 0–0 origins of the phosphorescence spectra obtained in EtOH at 77 K. [f] In powder.

spectra were found after 15 min irradiation. These results indicate that the prepared BF_2DKs are photochemically stable in solution. The absorption and fluorescence spectra in MeCN are deposited in the ESI as Fig. S1.† The shapes of the absorption spectra for the ChBs are similar to each other. All the compounds provided fluorescence spectra without vibrational structures in the solutions. The wavelengths (λ_{flu}) of the fluorescence maxima in $CHCl_3$ and MeCN are listed in Table 1. The fluorescence spectra in MeCN showed red shifts by 20–50 nm compared with those in $CHCl_3$, indicating that the fluorescence character of the studied BF_2DK is charge-transfer (CT). It is well known that pyrene shows intermolecular excimeric fluorescence in a concentrated solution.[41] At the studied concentration (~10^{-6} mol dm^{-3}), the observed fluorescence is not due to excimeric emission from 1-PyB. Because of the low solubility of 1-PyB in $CHCl_3$, we were unable to prepare highly concentrated solutions (>10^{-5} mol dm^{-3}). We found, however, that 1-PyB is soluble in DMSO, but excimeric fluorescence from 1-PyB was not observed in a concentrated DMSO solution (~10^{-3} mol dm^{-3}). The spectroscopic data in DMSO are deposited in the ESI as Fig. S2.† Phosphorescence at 77 K was recognized from the ChBs but not from 1-PyB. The triplet energies (E_T) of the ChBs were determined from the 0–0 origins of the phosphorescence spectra, and are listed in Table 1. The quantum yields (Φ_f) and lifetimes (τ_f) of the fluorescence in $CHCl_3$ and MeCN were determined, and are listed in Table 1. The decay profiles of the fluorescence for the studied BF_2DKs are deposited in the ESI as Fig. S3.† The decay profile of 1-PyB in MeCN was analyzed with a double exponential function, while the others were analyzed with a single exponential function. The origins of the double exponential decay profile of fluorescence for 1-PyB in MeCN, where excimeric fluorescence cannot be observed at the solution concentration, are not clear at present. The fluorescence rates (k_f), quantum yields (Φ_{nr}), and rate (k_{nr}) for the nonradiative processes were evaluated by eqn (1)–(3), respectively, except for 1-PyB in MeCN.

$$k_f = \Phi_f \tau_f^{-1} \quad (1)$$

$$\Phi_{nr} = 1 - \Phi_f \quad (2)$$

$$k_{nr} = \Phi_{nr} \tau_f^{-1} \quad (3)$$

The obtained rates are listed in Table 1.

Interestingly, the studied BF_2DKs emit intense fluorescence (Φ_f > *ca.* 0.8) in $CHCl_3$, although the fluorescence quantum yields in MeCN substantially decrease to 0.04 for 1-ChB and 1-PyB. The lifetime of fluorescence for 1-ChB in MeCN is also one-tenth shorter compared with that in $CHCl_3$, while that of 3-ChB shows a small variation in going from $CHCl_3$ to MeCN. According to eqn (2), we obtained the definite values of Φ_{nr}, indicating the presence of an internal conversion (IC) from the lowest excited singlet state (S_1) to the ground state (S_0) and intersystem crossing (ISC) from the S_1 to the lowest triplet state (T_1). The governing process of deactivating the S_1 state was revealed by transient absorption measurements using laser photolysis techniques, which will be mentioned later.

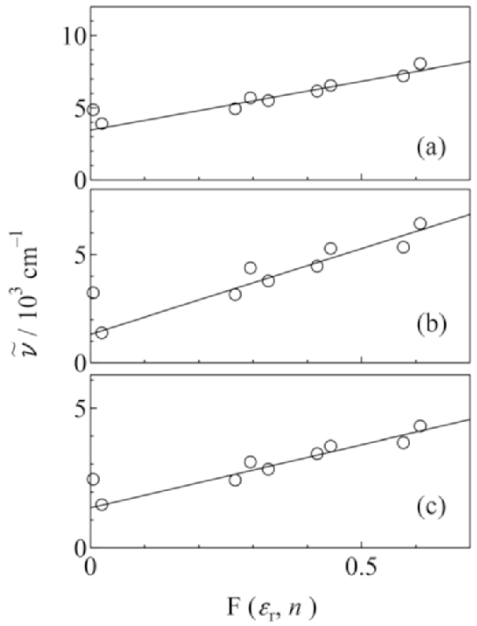

Fig. 2 The Lippert–Mataga plots for 1-ChB (a), 3-ChB (b) and 1-PyB (c). The lines were drawn by the least-squares best-fitting method.

Fig. 2 shows the Lippert–Mataga plots for the studied BF_2DKs, that is, the Stokes shifts, $\Delta\bar{\nu}$, defined by the energy difference between the first absorption band and the fluorescence maximum, plotted as a function of the solvent polarity parameter, the plots show slopes, indicating that the fluorescent states are of CT character. $F(\varepsilon_r, n)$ is defined by eqn (4) for the solvent using the relative dielectric constant, ε_r, and the refractive index, n.

$$F(\varepsilon_r, n) = 2(\varepsilon_r - 1)(2\varepsilon_r + 1)^{-1} - 2(n^2 - 1)(2n^2 + 1)^{-1} \quad (4)$$

The $\Delta\bar{\nu}$ values obtained in various solvents are listed in Tables S1–S3 in the ESI† along with the values of $F(\varepsilon_r, n)$ for the solvents used in the present study. The relationship between the Stokes shift, $\Delta\bar{\nu}$, and the solvent polarity, $F(\varepsilon_r, n)$, can be interpreted on the basis of the Lippert–Mataga equation:

$$\Delta\bar{\nu} = F(\varepsilon_r, n)(\mu_e - \mu_g)^2(4\pi\varepsilon_0 hca^3)^{-1} + \text{constant} \quad (5)$$

where μ_e, μ_g, ε_0, h, c, and a are, respectively, the dipole moments in the excited and ground states, the dielectric constants in vacuum, the Planck constant, velocity of light, and the Onsager radius of the BF_2DKs. Except for the plot for benzene, best-fitted straight lines are drawn in Fig. 2. The values of the intercept and the slope of the lines are listed in Table 2.

The Onsager radii, a, and the value for μ_g were obtained from the results of the DFT calculations for the optimized molecular structures in the ground state for the BF_2DKs. The $2a$ values were estimated to be equivalent to the distances between C8 and C4′ for the ChBs and between C7 and C4′ for 1-PyB (see Chart 1 for the position numbers). Based on the obtained values of the slope, a, and μ_g, the values for μ_e were determined. The values of a, μ_g, μ_e, and the absolute values of $\mu_e - \mu_g$ are listed in Table 2. The ratios (μ_e/μ_g) of μ_e to μ_g for the BF_2DKs can be used to assess the degree of CT character in the fluorescence state. It is noteworthy that the ratios for the ChBs are twice greater than that for 1-PyB (see Table 2).

Fig. 3 shows the fluorescence spectra in the solid state (powder) of the studied BF_2DKs. It is noteworthy that all the fluorescence maxima (λ_{flu}^{powder}) in the solid state, listed in Table 1, are red-shifted compared with those in solution. It is typically observed for the BF_2DKs that the wavelength of the emission band in solution differs from that in the solid state.[47] The fluorescence yields (Φ_f^{powder}) in powder were determined, and are listed in Table 1, as well as the λ_{flu}^{powder} values. The Φ_f^{powder} values (*ca.* 0.2) of 1-ChB and 1-PyB are similar to each other. The Φ_f^{powder} value of 3-ChB is one-quarter of that for 1-ChB, indicating that the fluorescence quantum yield of the ChBs in the solid state depends on the substitution position on the chrysene skeleton. We are unable to discuss their difference in the solid-state fluorescence behavior in detail because no single crystals of the present BF_2DKs suitable for X-ray diffraction analysis were obtained.

We carried out laser flash photolysis of the studied BF_2DKs to investigate the deactivation processes from the S_1 state. Fig. 4 shows the transient absorption spectra obtained upon 266 nm laser pulsing in the $CHCl_3$ solution of the BF_2DKs.

Transient absorption spectra were obtained in the wavelength region of 350–820 nm. The intensities of the transient absorption signals decreased with decay lifetimes (τ_T) in the microsecond time domain, and are listed in Table 1. The T–T absorption spectra in MeCN are deposited in the ESI as Fig. S4,† while the τ_T values in MeCN are also listed in Table 1. The τ_T values were shortened to 0.44 μs, 0.39 μs, and 0.42 μs for 1-ChB, 3-ChB, and 1-PyB in aerated $CHCl_3$, respectively, and to 0.34 μs for 3-ChB in aerated MeCN, indicating that the transient signals are ascribable to the triplet–triplet

Table 2 Analyzed data for the Lippert–Mataga plots for the BF_2DKs[a]

Compound	Intercept/10^3 cm^{-1}	Slope[b]/10^3 cm^{-1}	a/nm	$\mu_e - \mu_g$/Debye	μ_g/Debye	μ_e/Debye	μ_e/μ_g
1-ChB	3.46	6.78	0.783	24.70	7.09	31.79	4.5
3-ChB	1.32	7.91	0.827	28.96	7.24	36.20	5.0
1-PyB	1.43	4.52	0.678	16.25	9.93	26.18	2.6

[a] See text for details. [b] The regression coefficients were, respectively, 0.95, 0.92, and 0.94 for 1-ChB, 3-ChB and 1-PyB.

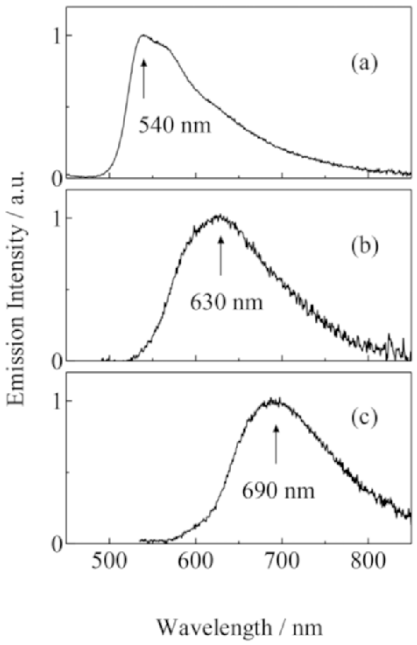

Fig. 3 Fluorescence spectra obtained in the solid state (powder) at 295 K for 1-ChB (a), 3-ChB (b) and 1-PyB (c).

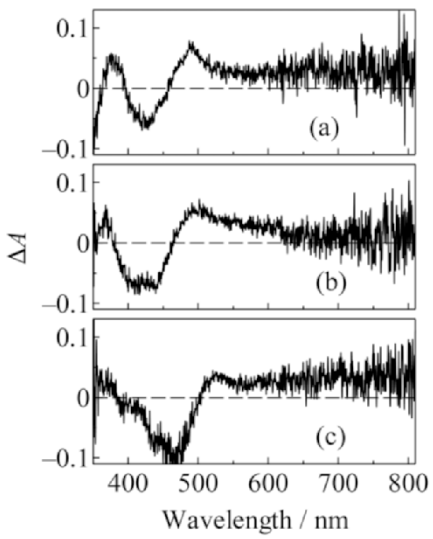

Fig. 4 Transient absorption spectra obtained at 200 ns upon 266 nm laser pulsing in the Ar-purged $CHCl_3$ solution of 1-ChB (a), 3-ChB (b) and 1-PyB (c) at 295 K.

(T–T) absorption. The shapes of the T–T absorption spectra in MeCN are similar to those in $CHCl_3$. These observations indicate that the triplet states have little CT character in solution, in contrast to the S_1 states. Observation of the triplet state in solution indicates that ISC from the S_1 to the T_1 state competes with the fluorescence process. The signal intensity of the T–T absorption in MeCN is substantially smaller than that in $CHCl_3$. From these facts, it can be inferred that the ISC quantum yields of the studied BF_2DKs in MeCN are smaller than those in $CHCl_3$. Considering that the Φ_{nr} values (0.7–0.96) in MeCN are greater than those (0.1–0.2) in $CHCl_3$, IC from the S_1 state to the ground state is operative in MeCN because of the CT character induced in polar media.

To obtain an insight into the photophysical properties of the BF_2DKs, density functional theory (DFT) was used to calculate the electronic structures, and time-dependent DFT (TD-DFT) was adopted to investigate the electronic transitions from the ground to the excitation states. All the calculations were performed at the B3LYP/6-31G(d) level with the Gaussian 09 program package.[44] The calculated results are summarized in Table 3.

Fig. 5 shows the calculated molecular orbital surfaces for the studied BF_2DKs showing the highest occupied molecular orbitals (HOMO) and lowest unoccupied molecular orbitals (LUMO) in $CHCl_3$. In the optimized structures of the studied BF_2DKs, the HOMO surfaces are mainly localized over the chrysene and pyrene moieties, respectively. The LUMO surfaces are mainly delocalized over the β-diketone backbone of the BF_2DKs. As the electronic surfaces are located on the different moieties between the HOMO and LUMO, the HOMO → LUMO transitions of the BF_2DKs responsible for the $S_0 \rightarrow S_1$ transition were characterized to be of CT. This assignment agrees with the results from the Lippert–Mataga analysis mentioned above. The evaluated *f* value (*ca.* 0.7) for 1-PyB is greater than those (*ca.* 0.2–0.35) for the ChBs. The difference in the *f* value between the ChBs and 1-PyB may be derived from the difference in the degree of the overlapping between the HOMO and the LUMO surfaces. Based on the Lippert–Mataga analysis and the TD-DFT results, the S_1 state of 1-PyB is not of a π,π* character, which is necessary for excimeric interaction. Presumably, excimeric fluorescence was not observed even in a high concentration solution for 1-PyB because of the absence of the π,π* transition character from the S_1 state.

Table 3 Calculated photophysical properties of the BF_2DKs in $CHCl_3$[a]

Compound	HOMO/eV	LUMO/eV	λ_{tr}[b]/nm	*f*[c]	Configuration coefficient[d]
1-ChB	−0.22228 (−0.22270)	−0.11407 (−0.11509)	498 (500)	0.2114 (0.2135)	0.70196 (0.70243)
3-ChB	−0.22398 (−0.22278)	−0.11627 (−0.11756)	493 (499)	0.3459 (0.3202)	0.70343 (0.70354)
1-PyB	−0.21917 (−0.21907)	−0.11535 (−0.11662)	508 (512)	0.6789 (0.6620)	0.70215 (0.70226)

[a] Data in parentheses are calculated results considering the dielectric constant of MeCN. [b] Wavelength estimated from the transition energy. [c] Oscillator strength for the $S_0 \rightarrow S_1$ transition. [d] For transitions from HOMO to LUMO.

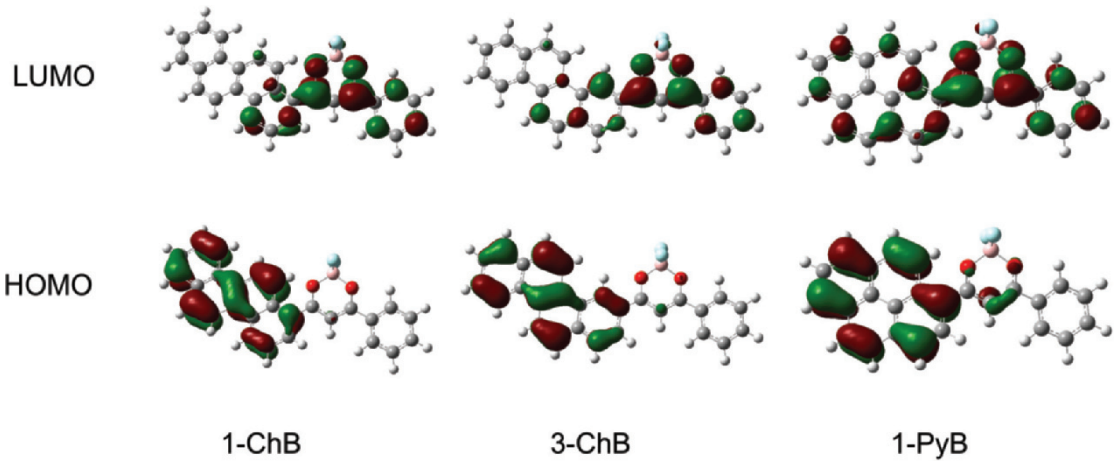

Fig. 5 The HOMO and LUMO surfaces for the studied BF_2DKs in $CHCl_3$.

4. Conclusion

We successfully prepared BF_2DKs with chrysene and pyrene moieties, and investigated their photophysical features in solution and in the solid state. The studied BF_2DKs were found to be photochemically stable in solution, and showed luminescence at 530–700 nm in powder, whereas green fluorescence in solution was observable, which underwent red shifts as the solvent polarity increased. Excimeric fluorescence from 1-PyB was not obtained even in a highly concentrated solution. The Φ_f values of the BF_2DKs decreased in polar solutions because of the enhanced IC process from the S_1 state with the CT character to the ground state. Laser photolysis studies of the BF_2DKs in solution revealed the formation of the T_1 states, which competes with the fluorescence and the IC processes. The studied BF_2DKs are potentially applicable for fluorophores in emission devices, *e.g.*, organic light emitting diodes, and such a study is currently underway.

Acknowledgements

This study has been supported by a Grant-in-Aid for Scientific Research (26288032) from the Ministry of Education, Culture, Sports, Science and Technology (MEXT) of Japanese Government. MY thanks the Cosmetrogy Research Foundation for the financial support. HO is grateful for the Okayama Foundation for Science and Technology. Prof. Fumito Tani at Kyusyu University is acknowledged for performing the HRMS spectrometry of the new compounds under Cooperative Research Program of the Network Joint Research Center for Materials and Devices.

References

1 K. Ono, K. Yoshikawa, Y. Tsuji, H. Yamaguchi, R. Uozumi, M. Tomura, K. Taga and K. Saito, Synthesis and photoluminescence properties of BF_2 complexes with 1,3-diketone ligands, *Tetrahedron*, 2007, **63**, 9354–9358.

2 A. G. Mirochnik, E. V. Gukhman, V. E. Karasev and P. A. Zhikhareva, Fluorescence and photochemical properties of crystalline boron difluorides β-diketonato, *Russ. Chem. Bull.*, 2000, **49**, 1024–1027.

3 A. Sakai, M. Tanaka, E. Ohta, Y. Yoshimoto, K. Mizuno and H. Ikeda, White light emission from a single component system: Remarkable concentration effects on the fluorescence of 1,3-diaroylmethanatoboron difluoride, *Tetrahedron Lett.*, 2012, **53**, 4138–4141.

4 Y. L. Chow and X. Cheng, 1,3-Diketonateboron difluoride sensitized cation radical reactions, *Can. J. Chem.*, 1991, **69**, 1331–1336.

5 Y. L. Chow and X. Cheng, The dual pathway in photocycloaddition of 1,3-diketonatoboron difluorides: Excimer reactions, *Can. J. Chem.*, 1991, **69**, 1575–1583.

6 Y. L. Chow and X. Ouyang, The photoaddition of 1,3-diketonatoboron difluorides with benzene derivatives, *Can. J. Chem.*, 1991, **69**, 423–431.

7 Y. L. Chow, X. Cheng and C. I. Johansson, Molecular interactions of dibenzoylmethanatoboron difluoride ($DBMBF_2$) in the excited and ground states in solution, *J. Photochem. Photobiol., A*, 1991, **57**, 247–255.

8 H. D. Ilge, E. Birckner, D. Fassler, M. V. Kozmenko, M. G. Kuz'min and H. Hartmann, Spectroscopy, photophysics and photochemistry of 1,3-diketoboronates: IV: Luminescence spectroscopic investigations of 2-naphthyl-substituted 1,3-diketoboronates, *J. Photochem.*, 1986, **32**, 177–189.

9 W. Schade, H. D. Ilge and H. Hartmann, Zur massenspektroskopischen charakterisierung von 1,3-diketoboraten mass spectroscopical studies on 1,3-diketoboronates, *J. Prakt. Chem.*, 1986, **328**, 941–944.

10 E. Cogné-Laage, J.-F. Allemand, O. Ruel, J.-B. Baudin, V. Croquette, M. Blanchard-Desce and L. Jullien, Diaroyl (methanato)boron difluoride compounds as medium-

sensitive two-photon fluorescent probes, *Chem. – Eur. J.*, 2004, **10**, 1445–1455.
11 L. A. Padilha, S. Webster, O. V. Przhonska, H. Hu, D. Peceli, T. R. Ensley, M. V. Bondar, A. O. Gerasov, Y. P. Kovtun, M. P. Shandura, A. D. Kachkovski, D. J. Hagan and E. W. V. Stryland, Efficient two-photon absorbing acceptor-π-acceptor polymethine dyes, *J. Phys. Chem. A*, 2010, **114**, 6493–6501.
12 C. Ran, X. Xu, S. B. Raymond, B. J. Ferrara, K. Neal, B. J. Bacskai, Z. Medarova and A. Moore, Design, synthesis, and testing of difluoroboron-derivatized curcumins as near-infrared probes for in vivo detection of amyloid-β deposits, *J. Am. Chem. Soc.*, 2009, **131**, 15257–15261.
13 C.-T. Poon, W. H. Lam, H.-L. Wong and V. W.-W. Yam, A versatile photochromic dithienylethene-containing β -diketonate llgand: Near-infrared photochromic behavior and photoswitchable luminescence properties upon incorporation of a boron(III) center, *J. Am. Chem. Soc.*, 2010, **132**, 13992–13993.
14 G. Zhang, J. Chen, S. J. Payne, S. E. Kooi, J. N. Demas and C. L. Fraser, Multi-emissive difluoroboron dibenzoylmethane polylactide exhibiting intense fluorescence and oxygen-sensitive room-temperature phosphorescence, *J. Am. Chem. Soc.*, 2007, **129**, 8942–8943.
15 G. Zhang, J. Lu, M. Sabat and C. L. Fraser, Polymorphism and reversible mechanochromic luminescence for solid-state difluoroboron avobenzone, *J. Am. Chem. Soc.*, 2010, **132**, 2160–2162.
16 T. Liu, A. D. Chien, J. Lu, G. Zhang and C. L. Fraser, Arene effects on difluoroboron β -diketonate mechanochromic luminescence, *J. Mater. Chem.*, 2011, **21**, 8401–8408.
17 K. Ono, J. Hashizume, H. Yamaguchi, M. Tomura, J.-I. Nishida and Y. Yamashita, Synthesis, crystal structure, and electron-accepting property of the BF_2 complex of a dihydroxydione with a perfluorotetracene skeleton, *Org. Lett.*, 2009, **11**, 4326–4329.
18 Y. Sun, D. Rohde, Y. Liu, L. Wan, Y. Wang, W. Wu, C. Di, G. Yu and D. Zhu, A novel air-stable n-type organic semiconductor: 4,4'-bis[(6,6'-diphenyl)-2,2-difluoro-1,3,2-dioxaborine] and its application in organic ambipolar field-effect transistors, *J. Mater. Chem.*, 2006, **16**, 4499–4503.
19 F. Jäkle, Borylated polyolefins and their applications, *J. Inorg. Organomet. Polym.*, 2005, **15**, 293–307.
20 F. Jäkle, Lewis acidic organoboron polymers, *Coord. Chem. Rev.*, 2006, **250**, 1107–1121.
21 F. Jäkle, Advances in the synthesis of organoborane polymers for optical, electronic, and sensory applications, *Chem. Rev.*, 2010, **110**, 3985–4022.
22 Y. Qin, I. Kiburu, S. Shah and F. Jäkle, Synthesis and characterization of organoboron quinolate polymers with tunable luminescence properties, *Macromolecules*, 2006, **39**, 9041–9048.
23 Y. Nagata, H. Otaka and Y. Chujo, Synthesis of new main-chain-type organoboron quinolate polymer linked on quinolate ligand, *Macromolecules*, 2008, **41**, 737–740.
24 A. Nagai, K. Kokado, Y. Nagata and Y. Chujo, 1,3-Diketone-based organoboron polymers: Emission by extending π-conjugation along a polymeric ligand, *Macromolecules*, 2008, **41**, 8295–8298.
25 A. Nagai and Y. Chujo, Luminescent organoboron conjugated polymers, *Chem. Lett.*, 2010, **39**, 430–435.
26 J. Samonina-Kosicka, C. A. DeRosa, W. A. Morris, Z. Fan and C. L. Fraser, Dual-emissive difluoroboron naphthylphenyl β -diketonate polylactide materials: Effects of heavy atom placement and polymer molecular weight, *Macromolecules*, 2014, **47**, 3736–3746.
27 D. R. G. Pitter, A. S. Brown, J. D. Baker and J. N. Wilson, One probe, two-channel imaging of nuclear and cytosolic compartments with orange and red emissive dyes, *Org. Biomol. Chem.*, 2015, **13**, 9477–9484.
28 C. A. DeRosa, J. Samonina-Kosicka, Z. Fan, H. C. Hendargo, D. H. Weitzel, G. M. Palmer and C. L. Fraser, Oxygen sensing difluoroboron dinaphthoylmethane polylactide, *Macromolecules*, 2015, **48**, 2967–2977.
29 T. Butler, W. A. Morris, J. Samonina-Kosicka and C. L. Fraser, Mechanochromic luminescence and aggregation induced emission of dinaphthoylmethane β -diketones and their boronated counterparts, *ACS Appl. Mater. Interfaces*, 2016, **8**, 1242–1251.
30 E. Kim, A. Felouat, E. Zaborova, J.-C. Ribierre, J. W. Wu, S. Senatore, C. Matthews, P.-F. Lenne, C. Baffert, A. Karapetyan, M. Giorgi, D. Jacquemin, M. Ponce-Vargas, B. L. Guennic, F. Fages and A. D'Aleo, Borondifluoride complexes of hemicurcuminoids as bio-inspired push–pull dyes for bioimaging, *Org. Biomol. Chem.*, 2016, **14**, 1311–1324.
31 L. F. Minuti, M. G. Memeo, S. Crespi and P. Quadrelli, Fluorescent probes from stable aromatic nitrile oxides, *Eur. J. Org. Chem.*, 2016, 821–829.
32 S. Xu, R. E. Evans, T. Liu, G. Zhang, J. N. Demas, C. O. Trindle and C. L. Fraser, Aromatic difluoroboron β -diketonate complexes: Effects of π-conjugation and media on optical properties, *Inorg. Chem.*, 2013, **52**, 3597–3610.
33 H. Okamoto, N. Kawasaki, Y. Kaji, Y. Kubozono, A. Fujiwara and M. Yamaji, Air-assisted high-performance field-effect transistor with thinfilms of picene, *J. Am. Chem. Soc.*, 2008, **130**, 10470–10471.
34 R. Mitsuhashi, Y. Suzuki, Y. Yamanari, H. Mitamura, T. Kambe, N. Ikeda, H. Okamoto, A. Fujiwara, M. Yamaji, N. Kawasaki, Y. Maniwa and Y. Kubozono, Superconductivity in alkali-metal-doped picene, *Nature*, 2010, **464**, 76–79.
35 H. Okamoto, M. Yamaji, S. Gohda, Y. Kubozono, N. Komura, K. Sato, H. Sugino and K. Satake, Facile synthesis of picene from 1,2-di(1-naphthyl)ethane by 9-fluorenone-sensitized photolysis, *Org. Lett.*, 2011, **13**, 2758–2761.
36 T. Itoh, M. Yamaji and H. Okamoto, S_2 fluorescence from picene vapor, *Chem. Phys. Lett.*, 2013, **570**, 26–28.
37 H. Okamoto, M. Yamaji, S. Gohda, K. Sato, H. Sugino and K. Satake, Photochemical synthesis and electronic spectra

of fulminene ([6]phenacene), *Res. Chem. Intermed.*, 2013, **39**, 147–159.

38 M. Yamaji, Y. Hakoda, A. Horimoto and H. Okamoto, Photochemical synthesis of diphenylphenanthrenes, and the photophysical properties studied by emission and transient absorption measurements, *Rapid Commun. Photosci.*, 2014, **3**, 73–75.

39 H. Okamoto, S. Hamao, H. Goto, Y. Sakai, M. Izumi, S. Gohda, Y. Kubozono and R. Eguchi, Transistor application of alkyl-substituted picene, *Sci. Rep.*, 2014, **4**, 5048–5053.

40 M. Mamiya, Y. Suwa, H. Okamoto and M. Yamaji, Preparation and photophysical properties of fluorescent difluoroboronated β -diketones having phenanthrene moieties studied by emission and transient absorption measurements, *Photochem. Photobiol. Sci.*, 2016, **15**, 278–286.

41 T. Förster and K. Kasper, Ein konzentrationsumschlag der fluoreszenz des pyrens, *Z. Elektrochem., Ber. Bunsen. Phys. Chem.*, 1955, **59**, 976–980.

42 F. B. Mallory and C. W. Mallory, *Org. React.*, 1983, **30**, 1–456.

43 M. Yamaji, Y. Aihara, T. Itoh, S. Tobita and H. Shizuka, Thermochemical profiles on hydrogen atom transfer from triplet naphthol and proton-induced electron transfer from triplet methoxynaphthalene to benzophenone via triplet exciplexes studied by laser flash photolysis, *J. Phys. Chem.*, 1994, **98**, 7014–7021.

44 M. J. Frisch, G. W. Trucks, H. B. Schlegel, G. E. Scuseria, M. A. Robb, J. R. Cheeseman, G. Scalmani, V. Barone, B. Mennucci, G. A. Petersson, H. Nakatsuji, M. Caricato, X. Li, H. P. Hratchian, A. F. Izmaylov, J. Bloino, G. Zheng, J. L. Sonnenberg, M. Hada, M. Ehara, K. Toyota, R. Fukuda, J. Hasegawa, M. Ishida, T. Nakajima, Y. Honda, O. Kitao, H. Nakai, T. Vreven, J. J. A. Montgomery, J. E. Peralta, F. Ogliaro, M. Bearpark, J. J. Heyd, E. Brothers, K. N. Kudin, V. N. Staroverov, T. Keith, R. Kobayashi, J. Normand, K. Raghavachari, A. Rendell, J. C. Burant, S. S. Iyengar, J. Tomasi, M. Cossi, N. Rega, J. M. Millam, M. Klene, J. E. Knox, J. B. Cross, V. Bakken, C. Adamo, J. Jaramillo, R. Gomperts, R. E. Stratmann, O. Yazyev, A. J. Austin, R. Cammi, C. Pomelli, J. W. Ochterski, R. L. Martin, K. Morokuma, V. G. Zakrzewski, G. A. Voth, P. Salvador, J. J. Dannenberg, S. Dapprich, A. D. Daniels, O. Farkas, J. B. Foresman, J. V. Ortiz, J. Cioslowski and D. J. Fox, *Gaussian 09, revision D.01*, Gaussian, Inc., Wallingford CT, 2010.

45 H. Okamoto, T. Takane, S. Gohda, Y. Kubozono, K. Sato, M. Yamaji and K. Satake, Efficient synthetic photocyclization for phenacenes using a continuous flow reactor, *Chem. Lett.*, 2014, **43**, 994–996.

46 S. Chandrasekhar and A. Shrinidhi, Chloral hydrate as a water carrier for the efficient deprotection of acetals, dithioacetals, and tetrahydropyranyl ethers in organic solvents, *Synth. Commun.*, 2014, **44**, 1904–1913.

47 A. Sakai, E. Ohta, Y. Yoshimoto, M. Tanaka, Y. Matsui, K. Mizuno and H. Ikeda, New fluorescence domain "excited multimer" formed upon photoexcitation of continuously stacked diaroylmethanatoboron difluoride molecules with fused π-orbitals in crystals, *Chem. – Eur. J.*, 2015, **21**, 18128–18137.

